Metrol. Meas. Syst., Vol. XVII (2010), No. 2, pp. 00–00

PAN POLSKA AKADEMIA NAUK

METROLOGY AND MEASUREMENT SYSTEMS

Index 330930, ISSN 0860-8229

www.metrology.pg.gda.pl

M&MS

COMPARATIVE ANALYSIS OF THREE ALGORITHMS FOR TWO-CHANNEL COMMON FREQUENCY SINEWAVE PARAMETER ESTIMATION: ELLIPSE FIT, SEVEN PARAMETER SINE FIT AND SPECTRAL SINC FIT

Pedro M. Ramos[1)], Fernando M. Janeiro[2)], Tomáš Radil[3)]

1) Instituto de Telecomunicações, Instituto Superior Técnico, Av. Rovisco Pais 1, 1049-001 Lisbon, Portugal (✉Pedro.Ramos@Lx.it.pt, +351 21 841 8485)

2) Instituto de Telecomunicações, Universidade de Évora, Rua Romão Ramalho 59, 7000-671 Évora, Portugal (fmtj@uevora.pt)

3) Instituto de Telecomunicações, Av. Rovisco Pais 1, 1049-001 Lisbon, Portugal (Tomas.Radil@Lx.it.pt)

Abstract

In this paper, a comparison analysis of three different algorithms for the estimation of sine signal parameters in two-channel common frequency situations is presented. The relevance of this situation is clearly understood in multiple applications where the algorithms have been applied. They include impedance measurements, eddy currents testing, laser anemometry and radio receiver testing for example. The three algorithms belong to different categories because they are based on different approaches. The ellipse fit algorithm is a parametric fit based on the XY plot of the samples of both signals. The seven parameter sine fit algorithm is a least-squares algorithm based on the time domain fitting of a single tone sinewave model to the acquired samples. The spectral sinc fit performs a fitting in the frequency domain of the exact model of an acquired sinewave on the acquired spectrum. Multiple simulation situations and real measurements are included in the comparison to demonstrate the weaknesses and strong points of each algorithm.

Keywords: sinewave parameter estimation, amplitude and phase measurements, seven parameter sine fit, ellipse fit, spectral sinc fit.

1. Introduction

Scientific and technological evolution depends on the ability to measure physical quantities with ever increasing accuracy. Researchers in the instrumentation and measurement field have produced both hardware and software innovations that enable very accurate measurements. Special attention has been given to signal processing algorithms such as the ones used to estimate the parameters of acquired sinewaves. The need for algorithms that allow the characterization of analog to digital converters led the IEEE to include in the 1057 standard [1] two algorithms that estimate sinewave parameters: the three-parameter sine fit and the four-parameter sine fit algorithms. The former is used to estimate the sinewave parameters when its frequency is known, while the last one is used when either the signal frequency or the sampling frequency are not accurately known.

For many applications, such as impedance measurements [2], eddy currents testing [3], laser anemometry [4], radio receiver testing [5] and measurements of active and reactive power under sinusoidal conditions [6, 7], there is a need to estimate the parameters of two common frequency sinewaves usually acquired simultaneously. To this end, an extension of the algorithms standardized in [1] was developed and is known as the seven-parameter sine fit algorithm [8], which uses the data from both channels and takes advantage of the fact that the frequency is the same for both sinewaves. This algorithm has since been adapted for efficient implementation in DSP systems [9]. A different approach, based on the X–Y plot of the two common frequency sinewaves has produced the ellipse fit algorithm [10], which has also been

Article history: received on Apr. 4, 2010; accepted on Jun. 8, 2010; available online on Jun. 16, 2010.

modified to be implemented in DSP applications [11]. Recently, a new algorithm called spectral sinc fit [12] has been developed to estimate the two sinewave parameters. It relies on the fitting of the exact theoretical spectrum of a windowed sinewave to the spectral content of the acquired sinewaves.

In this paper, the performance of the ellipse fit, seven-parameter sine fit and spectral sinc fit algorithms is analyzed and compared. Using extensive numerical simulations the accuracy and precision of the amplitude ratio and phase difference of the two sinewaves is studied as a function of signal to noise ratio, sine amplitudes and sine phase difference. For the sinc fit and sine fit algorithms, an analysis of the estimated frequency accuracy and precision is also performed. This analysis is not possible in the ellipse fit algorithm since the frequency is not estimated. The results are also compared to the Crámer-Rao lower bound of two common frequency sinewave parameter estimators, developed in [13]. The analysis and comparison of the three algorithms is complemented with measurement results of two acquired sinewaves with added noise. The multiple acquisitions are then processed by each algorithm to assess their accuracy in a practical situation.

The paper is divided into five sections including the Introduction and the Conclusions. In Section 2, a detailed overview of the three algorithms under analysis is given. Section 3 presents the results of the numerical simulations performed for each algorithm. A comparison between the three algorithms and the Crámer-Rao lower bound is also presented here. Finally, the measurement results are presented and analyzed in Section 4.

2. The algorithms

This section describes the three algorithms compared in this paper: ellipse fit; seven-parameter sine fit; and spectral sinc fit. The goal of these algorithms is to estimate the amplitudes D_i and phases ϕ_i of two acquired sinewaves modeled by:

$$u_i(t) = D_i \cos(2\pi f t + \phi_i) + C_i = A_i \cos(2\pi f t) + B_i \sin(2\pi f t) + C_i, \tag{1}$$

where i is the channel number (i =1, 2), A_i is the in-phase and B_i the quadrature component of each sinewave. Some algorithms also estimate the DC components C_i and the common frequency f.

In most two-channel applications the value of the amplitude and phase of each signal is not required. The only values needed are the amplitude ratio D_2/D_1 and phase difference $\Delta\varphi = \phi_2 - \phi_1$. However, some algorithms require that the frequency f must also be estimated since it is not accurately known. This is due to the uncertainty of the generated sinewaves frequency f and uncertainty of the sampling frequency f_s.

The Cramér-Rao lower bounds (CRLB) for parameter estimation of dual-channel common frequency sinewaves was determined in [13] for an unbiased estimator under a Gaussian assumption using the signal to noise ratio defined as:

$$\mathrm{SNR}_i = \frac{D_i^2}{2\sigma_i^2}, \tag{2}$$

where σ_i^2 is the variance of the zero-mean Gaussian white noise of signal i.

For the relative amplitude ratio, the standard deviation that corresponds to the CRLB is:

$$\frac{\sigma_{D_2/D_1}}{D_2/D_1} = \sqrt{\frac{\mathrm{SNR}_1 + \mathrm{SNR}_2}{N\,\mathrm{SNR}_1\,\mathrm{SNR}_2}}, \tag{3}$$

while the standard deviation that corresponds to the bound of the phase difference is:

$$\sigma_{\Delta\varphi}[^\circ] = \frac{180}{\pi}\sqrt{\frac{\mathrm{SNR}_1 + \mathrm{SNR}_2}{N\,\mathrm{SNR}_1\,\mathrm{SNR}_2}} \tag{4}$$

and the normalized standard deviation that corresponds to the bound of the estimated frequency is:

$$\sigma_{\frac{f}{f_S}} = \sqrt{\frac{12}{(2\pi)^2 N^3 \left(\mathrm{SNR}_1 + \mathrm{SNR}_2\right)}}. \tag{5}$$

In this section, the sinewave parameter extraction is illustrated for each of the three algorithms using two simulated sinewaves sampled at $f_S = 96\ \mathrm{kS/s}$ with N = 200 samples. The waves parameters are D_1 = 1 V, D_2 = 0.25 V, $f = 1\ \mathrm{kHz}$ and $\Delta\varphi = 25^\circ$. A signal to noise ratio SNR = 30 dB was considered in both sinewaves.

2.1. Ellipse Fit

The ellipse fit algorithm was first developed in [14] and improved for numerical stability in [10]. It was then proposed as a non-iterative procedure to estimate the amplitudes and phase difference of two common frequency sinewaves [15].

The time dependence of the sinewaves can be discarded by parametrically plotting the two sinewaves in a XY plot, creating a Lissajous curve. Since the two sinewaves have the same frequency, the figure will be an ellipse, except when the two waveforms are in phase or opposition which makes the ellipse degenerate into a straight line.

Algebraically, the time dependence in (1) can be eliminated by rewriting them as:

$$\left(\frac{u_1}{D_1}\right)^2 + \left(\frac{u_2}{D_2}\right)^2 - 2\left(\frac{u_1 u_2}{D_1 D_2}\right)\cos(\Delta\varphi) - \sin^2(\Delta\varphi) = 0, \tag{6}$$

which is the ellipse equation. This corresponds to the general conic [9]:

$$F(u_1, u_2) = a u_1^2 + b u_1 u_2 + c u_2^2 + d u_1 + e u_2 + g = 0 \tag{7}$$

with the constraint $\Delta = b^2 - 4ac < 0$ so that the conic is an ellipse which corresponds to $\Delta\varphi \neq n\pi$ with $n \in \mathbb{Z}$. This constraint can be, by scaling of the conic (7), transformed into $b^2 - 4ac = -1$.

The conic model (7) is fitted to the sinewave data by a non-iterative constrained minimization process based on Lagrange multipliers [10], which yields the model parameters $[a, b, c, d, e, g]$. The sine amplitudes are given by:

$$D_1 = \frac{1}{\sqrt{ka}}, \qquad D_2 = \frac{1}{\sqrt{kc}}, \tag{8}$$

where k is the scaling factor to ensure $b^2 - 4ac = -1$. The phase difference $\Delta\varphi$ can be determined by:

$$\cos(\Delta\varphi) = -\frac{\mathrm{sign}(a)\,b}{2\sqrt{ac}}, \tag{9}$$

while its sign is obtained by observing the rotation direction of the ellipse. To avoid errors due to the presence of noise, a voting system was implemented to determine the rotation direction as described in [11].

The amplitude ratio D_2/D_1 is:

$$\frac{D_2}{D_1} = \sqrt{\frac{a}{c}} \tag{10}$$

and is independent of the scaling factor k.

Fig. 1 illustrates the ellipse fit procedure with the two sampled sinewaves plotted in an XY plot. The dots represent the noisy sinewave data points and the line shows the ellipse fitted by the procedure described above.

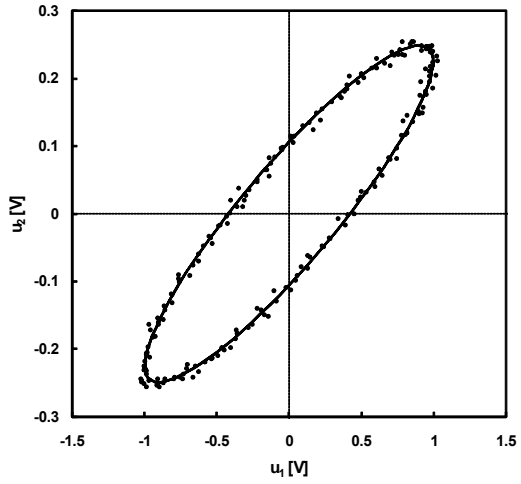

Fig. 1. Ellipse fit of two sinewaves with $D_1 = 1$ V, $D_2 = 0.25$ V, $f = 1$ kHz, $\Delta\varphi = 25^\circ$ and $N = 200$. The dots represent the sampled data and the line represents the fitted ellipse.

The original ellipse fit implementation [10] was modified in [15] to require only the construction of 3×3 matrices with a total of only 18 different elements (floats) independently of the number of samples. This is a major advantage in terms of memory requirements of the algorithm.

2.2. Seven-parameter sine fit

Sine fitting algorithms were standardized in [1] for ADC characterization. In the three-parameter version, the amplitude, phase and DC component of an acquired sinewave, of known frequency, are estimated in a non-iterative least-squares procedure. Since in most cases the frequency is not accurately known, the four-parameter sine fit version estimates the sinewave amplitude, DC component and phase along with its frequency. In this case the algorithm becomes non-linear and an iterative non-linear least-squares procedure is needed. The three- and four-parameter sine fit algorithms are suitable for single-channel data and can be independently applied to multi-channel data.

The seven-parameter sine fit algorithm was developed as an extension of the four-parameter algorithm for dual channel applications where the two signals have the same frequency [8]. In each iteration m the algorithm estimates the sinewave parameters $\mathbf{x}^{(m)} = \left[A_1^{(m)} \; B_1^{(m)} \; C_1^{(m)} \; \Delta f^{(m)} \; A_2^{(m)} \; B_2^{(m)} \; C_2^{(m)} \right]$, where $\Delta f^{(m)}$ is the frequency correction for the current iteration. These estimates are obtained from:

$$\mathbf{x}^{(m)} = \left[\left(\mathbf{D}^{(m-1)}\right)^T \mathbf{D}^{(m-1)}\right]^{-1}\left[\left(\mathbf{D}^{(m-1)}\right)^T \mathbf{y}\right], \tag{11}$$

where $\mathbf{y} = \left[u_{1,1}\, u_{1,2} \ldots u_{1,N}\, u_{2,1}\, u_{2,2} \ldots u_{2,N}\right]^T$ contains N samples of both signals and

$$\mathbf{D}^{(m-1)} = \begin{bmatrix} \mathbf{Q}_1^{(m-1)} & \mathbf{p}_1^{(m-1)} & \mathbf{0}_{N,3} \\ \mathbf{0}_{N,3} & \mathbf{p}_2^{(m-1)} & \mathbf{Q}_2^{(m-1)} \end{bmatrix}, \tag{12}$$

where $\mathbf{0}_{N,3}$ is a $N\times3$ zero matrix and

$$\mathbf{Q}_i^{(m-1)} = \begin{bmatrix} \cos\left(\beta_{i,1}\right) & \sin\left(\beta_{i,1}\right) & 1 \\ \cos\left(\beta_{i,2}\right) & \sin\left(\beta_{i,2}\right) & 1 \\ \vdots & \vdots & \vdots \\ \cos\left(\beta_{i,N}\right) & \sin\left(\beta_{i,N}\right) & 1 \end{bmatrix}, \quad \mathbf{p}_i^{(m-1)} = \begin{bmatrix} \alpha_{i,1} \\ \alpha_{i,2} \\ \vdots \\ \alpha_{i,N} \end{bmatrix} \tag{13}$$

with $\beta_{i,n} = \omega^{(m-1)} t_{i,n}$ and $\alpha_{i,n} = -2\pi A^{(m-1)} t_{i,n} \sin\left(\beta_{i,n}\right) + 2\pi B^{(m-1)} t_{i,n} \cos\left(\beta_{i,n}\right)$ where $t_{i,n}$ are the timestamps of signal i.

The initial estimates are obtained from the interpolated Discrete Fourier Transform (IpDFT) which yields a good frequency estimation [16]. The three-parameter algorithm is then used in each signal to estimate the remaining 6 initial parameters. The iterative procedure terminates when a predefined maximum number of iterations is reached (nonconvergence) or the relative frequency correction $\Delta f / f$ is below a certain threshold (convergence).

In Fig. 2, the sampled sinewaves are shown with dots (for u_1) and crosses (for u_2) while the sinewaves reconstructed with the parameters estimated by the sine fit algorithm are shown by continuous lines.

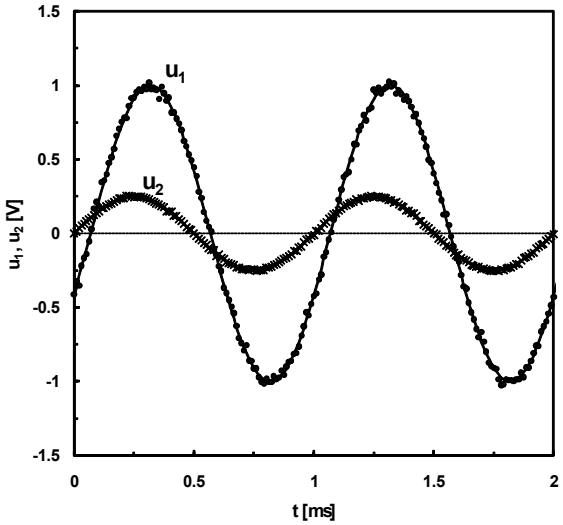

Fig. 2. Seven-parameter sine fit of two sinewaves with $D_1 = 1$ V, $D_2 = 0.25$ V, $f = 1$ kHz, $\Delta\varphi = 25^\circ$ and $N = 200$. The dots represent the u_1 sampled data, the crosses represent the u_2 sampled data and the lines represent the reconstructed sinewaves.

This algorithm involves the creation of a matrix of $2N\times7$ floating-point numbers. As the number of samples increases, the memory requirements will limit the algorithm applicability

in a DSP implementation. In [9], a more efficient version is presented that requires only 3*N*+63 floating-point memory positions.

2.3. Spectral sinc fit

The spectral sinc fit algorithm has been recently proposed as a new method to estimate the parameters of an acquired sinewave [12]. The method is based on fitting the theoretical frequency spectrum on the spectrum of the measured signals. The spectral sinc fit method has been extended to be applied to two-channel common frequency acquisitions.

The acquisition of a limited number of samples is equivalent to applying a rectangular window to the sinewaves. The theoretical spectrum of such a sinewave is [12]:

$$\hat{X}_i[k] = D_i P_i[k] = \frac{D_i}{2}\left[W\left(2\pi\frac{k}{N} - 2\pi\frac{f}{f_S}\right)e^{j\phi_i} + W\left(2\pi\frac{k}{N} + 2\pi\frac{f}{f_S}\right)e^{-j\phi_i}\right], \tag{14}$$

where $k \in [-N/2+1;\ N/2]$ and $W(\omega)$ is the spectrum of a rectangular window; *i.e.*, an aliased sinc function:

$$W(\omega) = \frac{\sin\left(\frac{\omega}{2}N\right)}{\sin\left(\frac{\omega}{2}\right)} e^{j\frac{\omega}{2}(N-1)}. \tag{15}$$

The resulting two-sided spectrum $\hat{X}_i[k]$ consists of two overlapping aliased sinc functions centered at $\pm\omega_X = \pm 2\pi f / f_s$. The maximums of $\hat{X}_i[k]$ are not centered at the frequencies $\pm\omega_X$ due to the leakage of one sinc into the other. Note that in the model (14), the DC component C_i is not included since in most applications it is not important (it does not carry information about the measured quantity).

The algorithm searches for the sinewaves parameters that minimize the cost functions:

$$\varepsilon_i = \sum_{k=k_{\max}-1}^{k_{\max}+1}\left[\left(D_i P_{i,\mathrm{Re}}[k] - X_{i,\mathrm{Re}}[k]\right)^2 + \left(D_i P_{i,\mathrm{Im}}[k] - X_{i,\mathrm{Im}}[k]\right)^2\right], \tag{16}$$

where $X_i[k]$ is the spectrum of each acquired signal.

From (16) it can be seen that the cost functions are evaluated in only three points of the spectrum, the point where the measured amplitude spectrum $|X_i[k]|$ has its maximum ($k_{\max}$) and the two neighboring points.

The algorithm exploits the fact that the relation between the theoretical spectrum $\hat{X}_i[k]$ and the amplitude D_i is linear (see (14)) to reduce the number of estimated parameters to three: two phases and the common frequency. The amplitude D_i is then calculated using the estimated parameters:

$$D_i = \frac{\sum_{k=k_{\max}-1}^{k_{\max}+1}\left(P_{i,\mathrm{Re}}[k]X_{i,\mathrm{Re}}[k] + P_{i,\mathrm{Im}}[k]X_{i,\mathrm{Im}}[k]\right)}{\sum_{k=k_{\max}-1}^{k_{\max}+1}\left(P_{i,\mathrm{Re}}^2[k] + P_{i,\mathrm{Im}}^2[k]\right)}. \tag{17}$$

The search for the minimums is an iterative procedure that uses the Gauss-Newton method. The initial frequency estimate is obtained by the IpDFT [16] and the remaining initial parameters are obtained by applying the three-parameter sine fit to each measured signal.

In order to compensate for the possible different signal to noise ratios in each of the two measured signals (due to *e.g.*, noise, spurious components, harmonic distortions), in each iteration weights are assigned to each signal and used in the Gauss-Newton method:

$$\begin{bmatrix} \phi_1^{(m)} \\ \phi_2^{(m)} \\ f^{(m)} \end{bmatrix} = \begin{bmatrix} \phi_1^{(m-1)} \\ \phi_2^{(m-1)} \\ f^{(m-1)} \end{bmatrix} - \left[\mathbf{J}^{(m-1)}\right]^{\dagger} \left(\frac{1}{\max\left(w_1, w_2\right)} \begin{bmatrix} w_1\mathbf{I}_6 & \mathbf{0}_{6,6} \\ \mathbf{0}_{6,6} & w_2\mathbf{I}_6 \end{bmatrix} \begin{bmatrix} \mathbf{r}_{1,\mathrm{Re}}^{(m-1)} \\ \mathbf{r}_{1,\mathrm{Im}}^{(m-1)} \\ \mathbf{r}_{2,\mathrm{Re}}^{(m-1)} \\ \mathbf{r}_{2,\mathrm{Im}}^{(m-1)} \end{bmatrix} \right), \tag{18}$$

where w_i are the weights, $\mathbf{I}_6$ is a 6×6 identity matrix, $\mathbf{0}_{6,6}$ is a 6×6 zero matrix, $\left[\mathbf{J}\right]^{\dagger}$ is the pseudo-inverse of the Jacobian matrix $\mathbf{J}$, the superscript (m) denotes the iteration number and $\mathbf{r}_i$ are the fitting residuals:

$$\mathbf{r}_i^{(m-1)} = \begin{bmatrix} D_i^{(m-1)} P_i^{(m-1)}\left[k_{\max} - 1\right] - X_i\left[k_{\max} - 1\right] \\ D_i^{(m-1)} P_i^{(m-1)}\left[k_{\max}\right] - X_i\left[k_{\max}\right] \\ D_i^{(m-1)} P_i^{(m-1)}\left[k_{\max} + 1\right] - X_i\left[k_{\max} + 1\right] \end{bmatrix}. \tag{19}$$

The weights w_i are the LS errors, calculated in the time domain as the difference between the measured signal and the signal reconstructed using the current estimates of the parameters.

The search ends when the relative change of the frequency estimate drops below a threshold or when the preset maximum number of iterations is exceeded. The weights w_i are used to estimate the Cramér-Rao lower bound (CRLB) of frequency estimation [13] which is then used to adjust the threshold level. This adaptive setting of the threshold level has an advantage over using a fixed setting because it prevents the threshold level to be set unrealistically low (below the CRLB) or too high.

The main advantage of this algorithm is that the iterative part can be accurately computed using as little as three sample points per signal (the three values of k in (16)) making it memory wise very efficient since only the initial FFTs are done with the full number of acquired samples.

Fig. 3 shows an example of amplitude spectrums of two sampled sinewaves and the spectrums that were fitted on them.

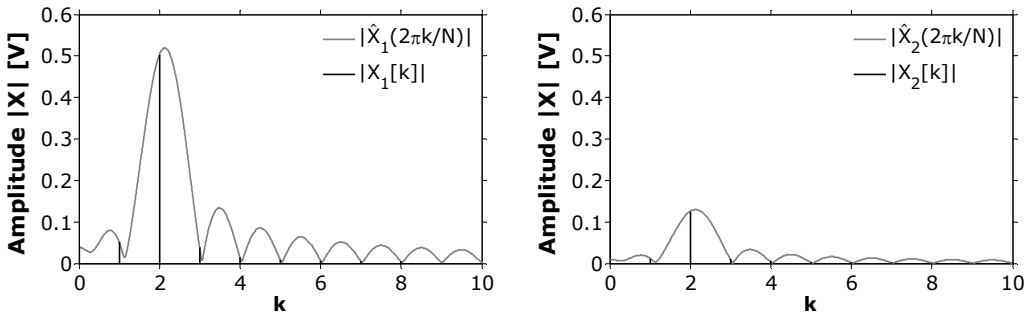

Fig. 3. Spectral sinc fit: positive frequencies of the two-sided amplitude spectrums of two sinewaves (D_1 = 1 V, D_2 = 0.25 V, f = 1 kHz, $\Delta\varphi = 25^{\circ}$ and N = 200) and the fitted spectrum.

3. Numerical simulations

To assess the performance of the three algorithms, they were implemented in Matlab and several tests were executed. Since the ultimate goal is to estimate the amplitude ratio (D_2/D_1) and the phase difference ($\Delta\varphi$), the tests estimated the amplitude ratio error (i.e., the difference between the estimated amplitude ratio and the imposed ratio) as well as the phase difference error. For each set of tested parameters, 100 000 different runs were executed to obtain the average values and the corresponding standard deviations. In each run, the initial phase of the first signal (ϕ_1) is a random variable with a uniform pdf between -180º and 180º. Signal frequency is 1 kHz and 1920 samples per channel are taken at 96 kS/s. White Gaussian noise is added according to each signal's signal-to-noise-ratio (SNR).

3.1. Signal to noise ratio analysis

In this analysis, the signal amplitudes are fixed at D_1=1 V and D_2=0.25 V. Since it is known that the ellipse fit algorithm cannot work near $\Delta\varphi$=180° and $\Delta\varphi$=0° because of ellipse degeneration, the phase difference is a uniform pdf in the $\pm[10^{\circ};170^{\circ}]$ range. This issue will be analyzed and discussed in Section 3.3.

The results for the ellipse fit are shown in Fig. 4 and Fig. 5. It can be seen that the algorithm is biased for signal to noise ratios typically below 40 dB. As expected, the standard deviations are reduced with the increase in SNR.

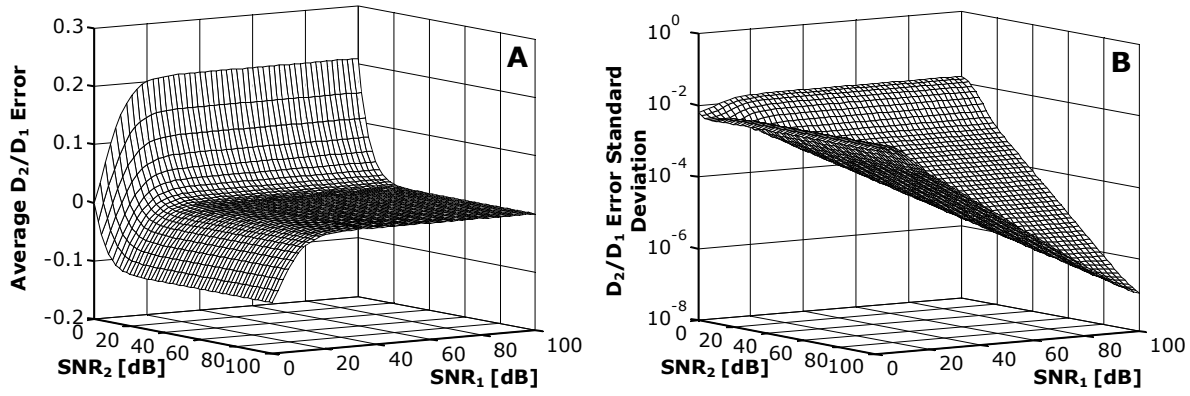

Fig. 4. Average amplitude ratio error (A) and corresponding standard deviation (B) for the ellipse fit algorithm as a function of the two signal to noise ratios for D_1=1 V and D_2=0.25 V.

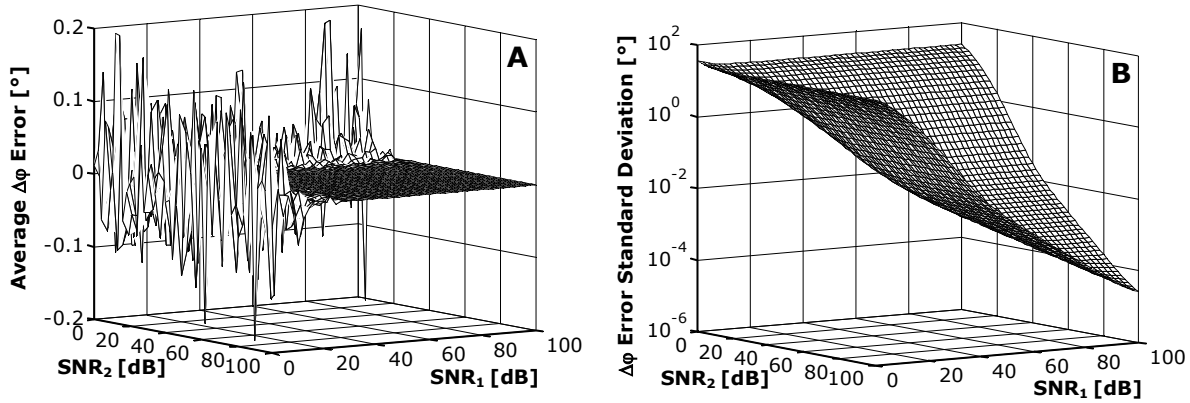

Fig. 5. Average phase difference error (A) and corresponding standard deviation (B) for the ellipse fit algorithm as a function of the two signal to noise ratios for D_1=1 V and D_2=0.25 V.

Note that the fluctuations in the results of the average phase errors (Fig. 5A) for the lowest signal to noise ratios are caused by the finite number of repetitions and that the corresponding standard deviations are considerably higher than the represented fluctuation (*e.g.*, for SNR=30 dB the average error is -0.005° and the standard deviation is 0.4°).

The results for the seven parameter sine fit are shown in Fig. 6 while the results for the spectral sinc fit are presented in Fig. 7. These algorithms are not biased and so the shown results correspond only to the standard deviations. Note that the evolutions of the standard deviations are quite similar for these algorithms. Comparing with the ellipse fit algorithm, the evolution pattern is the same, but the standard deviations are higher for the ellipse fit.

In Fig. 8, the relative standard deviation of the estimated frequency error is shown for the seven-parameter sine fit and for the spectral sinc fit (*i.e.*, for the algorithms that also estimate the signal frequency). It can be seen that the results of both algorithms are in the same order of magnitude but with considerable shape differences. This is caused by the fact that the sinc fit uses the information from the signal to noise ratios it estimates in order to weigh the information from the two signals giving more relevance to the signal with the highest SNR. This means that if one signal has a high SNR it will assure a very good frequency estimate without being influenced by the samples of the signal with the lower SNR. On the other hand, in the seven-parameter sine fit the residuals of both signals are not weighted and contribute equally to the estimates. In this case, if one signal has a high SNR and the other has a low SNR (and both have similar order of magnitude amplitudes as is the case in Fig. 8), the seven-parameter sine fit will assign equal weights to the signals and the signal with the lowest SNR will infect the frequency estimation causing a higher standard deviation.

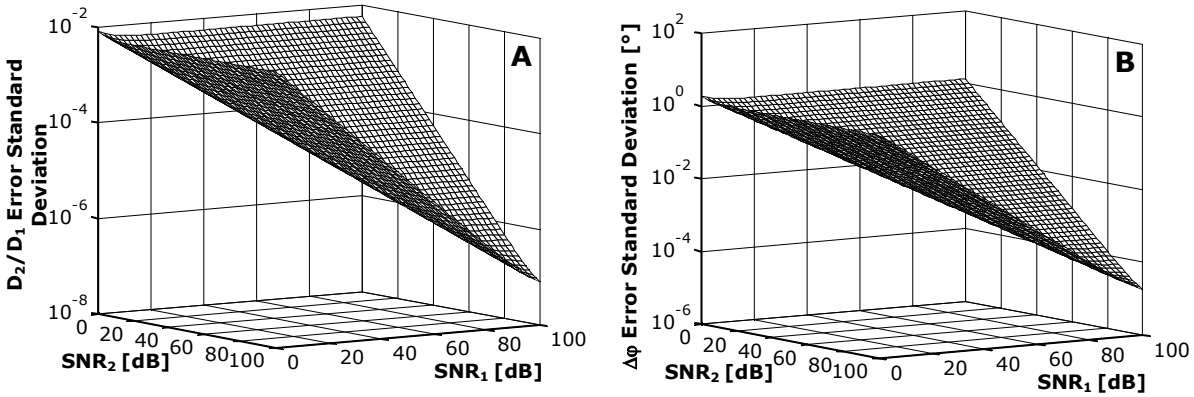

Fig. 6. Standard deviation of the amplitude ratio (A) and phase difference error (B) for the seven parameter sine fit algorithm as a function of the two signal to noise ratios for D_1=1 V and D_2=0.25 V.

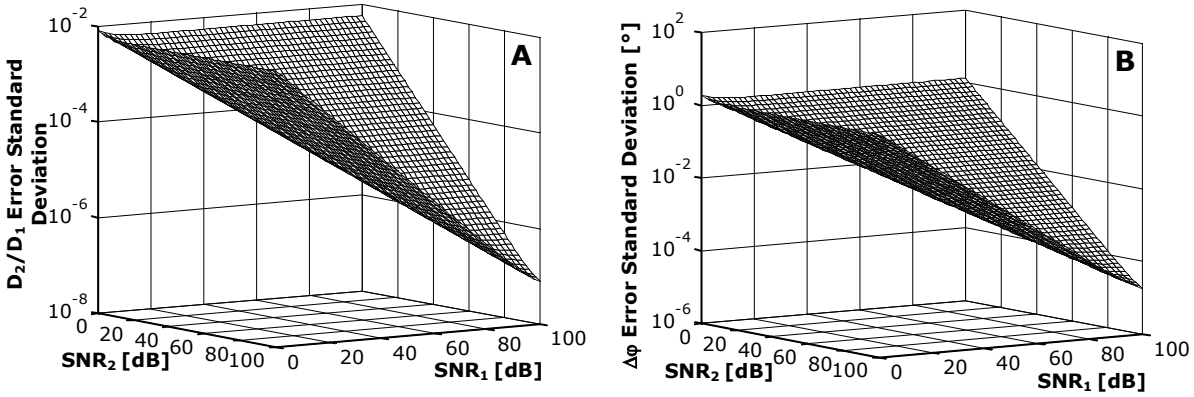

Fig. 7. Standard deviation of the amplitude ratio (A) and phase difference error (B) for the spectral sinc fit algorithm as a function of the two signal to noise ratios for D_1=1 V and D_2=0.25 V.

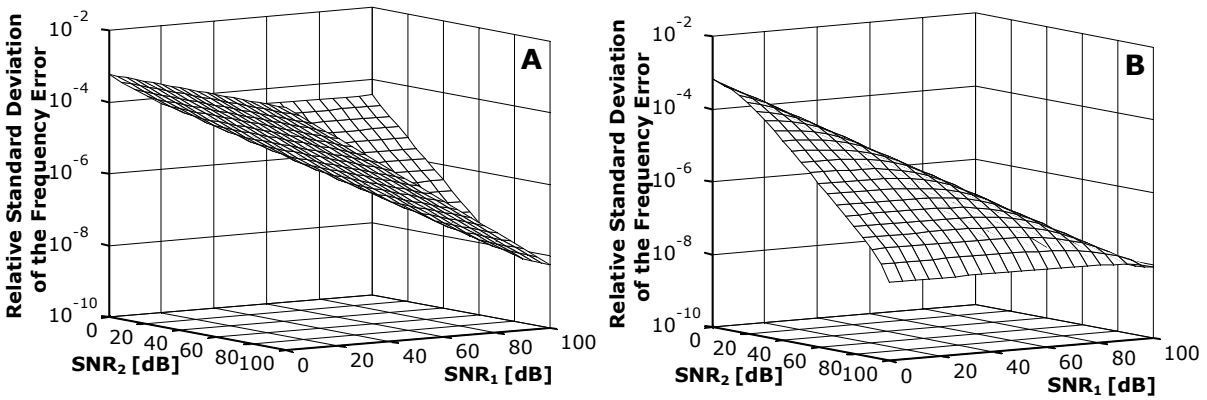

Fig. 8. Relative standard deviation of the estimated frequency error for the seven parameter sine fit algorithm (A) and for the spectral sinc fit algorithm (B) as a function of the two signal to noise ratios for D_1=1 V and D_2=0.25 V.

3.2. Amplitude analysis

In this section, the amplitude analysis of the three algorithms is presented. The signal to noise ratios are set to SNR_1 = 40 dB, SNR_2 = 80 dB and the amplitudes are swept from 0.1 V up to 2 V with 0.1 V resolution. In Fig. 9 the results corresponding to the amplitude ratio error standard deviation are presented for the three algorithms. Clearly, the results do not depend on the amplitudes but rather on the SNR of the signals. Comparing the three algorithms it can be seen that the spectral sinc fit results are identical to the seven-parameter algorithm results while the results obtained with the ellipse fit are a little higher.

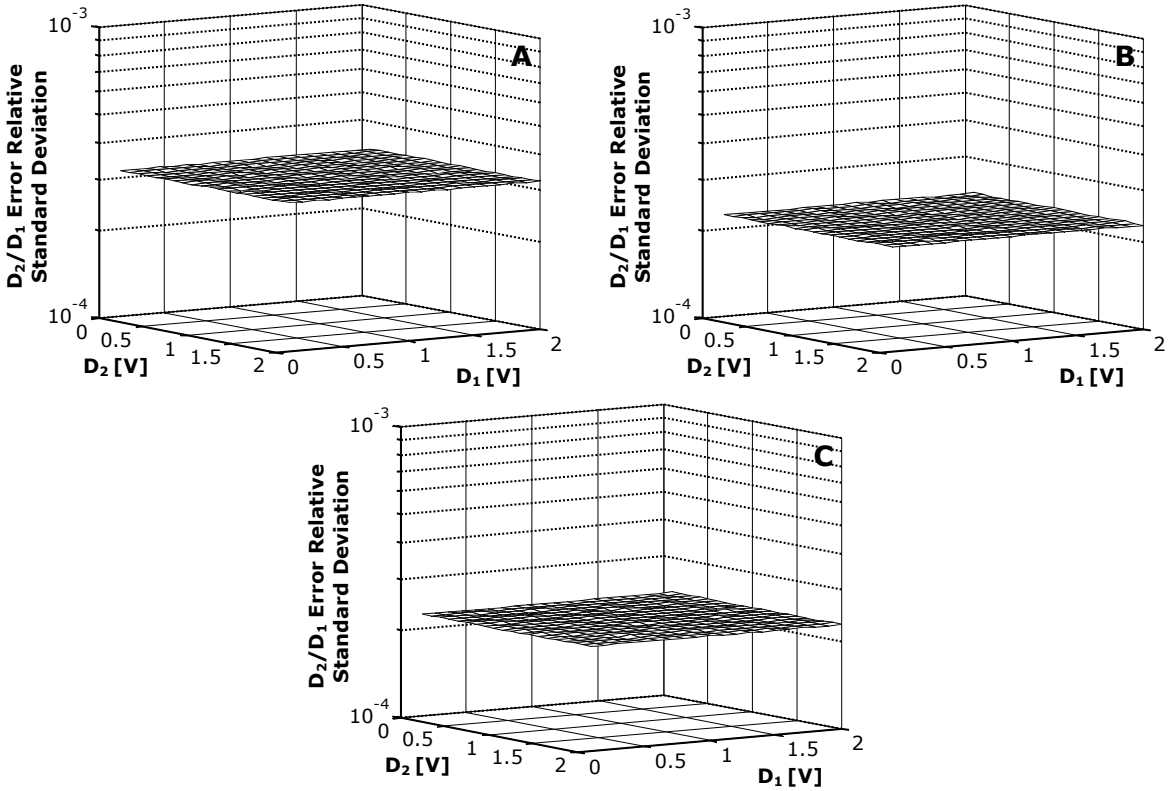

Fig. 9. Relative standard deviation of the amplitude ratio for the ellipse fit (A), seven parameter sine fit (B) and spectral sinc it (C) as a function of the two signal amplitudes for SNR_1=40 dB and SNR_2=80 dB.

In Fig. 10, the corresponding results for the phase error standard deviation are presented. Once again, the results of the spectral sinc fit and the seven-parameter sine fit are identical and the results of the ellipse fit algorithm are slightly worse. In the three cases, the results do not depend on the signal amplitude but rather on the signal SNRs.

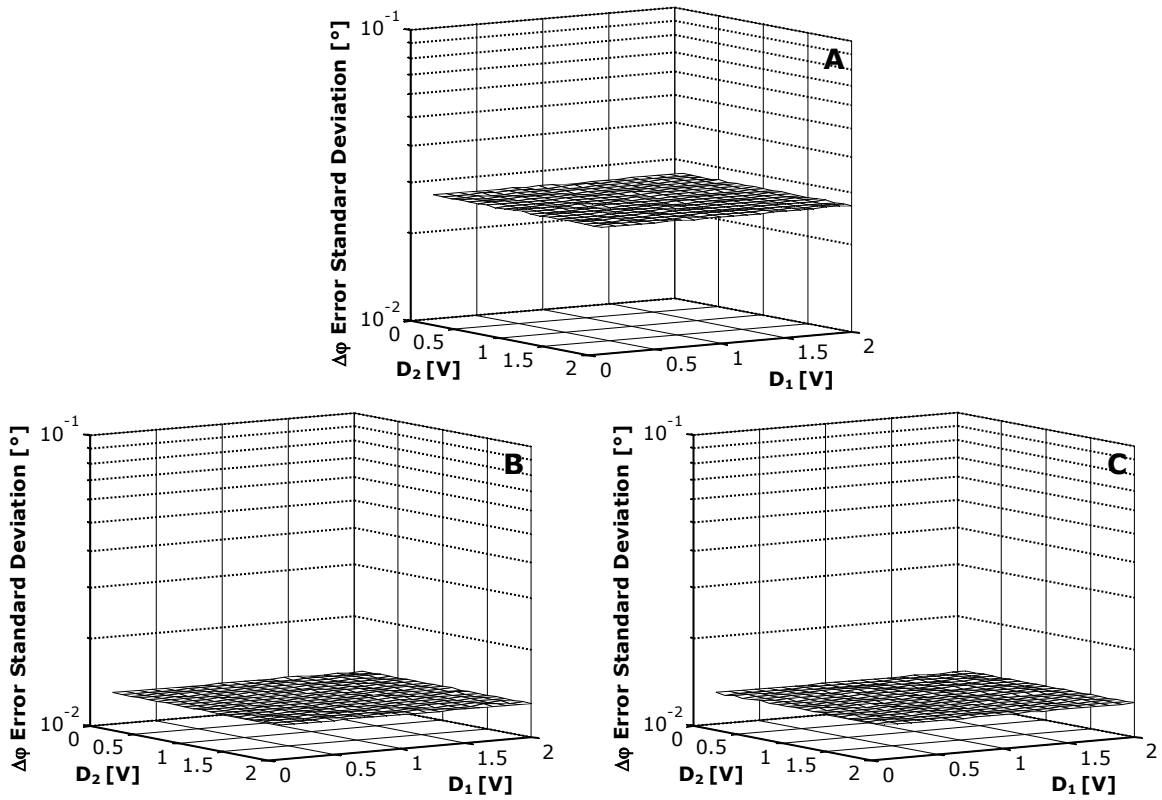

Fig. 10. Standard deviation of the estimated phase error for the ellipse fit (A), seven parameter sine fit (B) and spectral sinc fit (C) as a function of the two signal amplitudes for SNR_1=40 dB and SNR_2=80 dB.

3.3. Phase analysis

Regarding the phase analysis, the tests that were performed used D_1=1 V, D_2=0.5 V and three different values of the common SNR. The imposed phase difference was swept from -180º up to 180º with 0.005º resolution. As expected, the seven-parameter sine fit and the spectral sinc fit algorithms are independent on the phase difference (results presented in Table 1).

The ellipse fit algorithm is quite different. Due to ellipse degeneration, the algorithm has problems for phase differences near 0º and 180º (as shown in Fig. 11 and with more detail in Fig. 12 - note that the peak value differences between Fig. 11A and 12A are caused by the lower phase resolution in Fig. 11A). The range of affected phase difference values depends on the SNR values. Remarkably, in spite of the ellipse degeneration, the algorithm is capable of estimating the amplitude ratio without bias and with the same standard deviation for all phase difference values.

The results presented in Table 1 correspond to the values obtained with the three different algorithms for different values of signal to noise ratios and for the phase difference of 90º (to avoid problems with the ellipse fit algorithm), D_1=1 V and D_2=0.5 V. For comparison, the Cramér-Rao lower bounds, determined using the equations (2)-(4) derived in [13], are also included in Table 1.

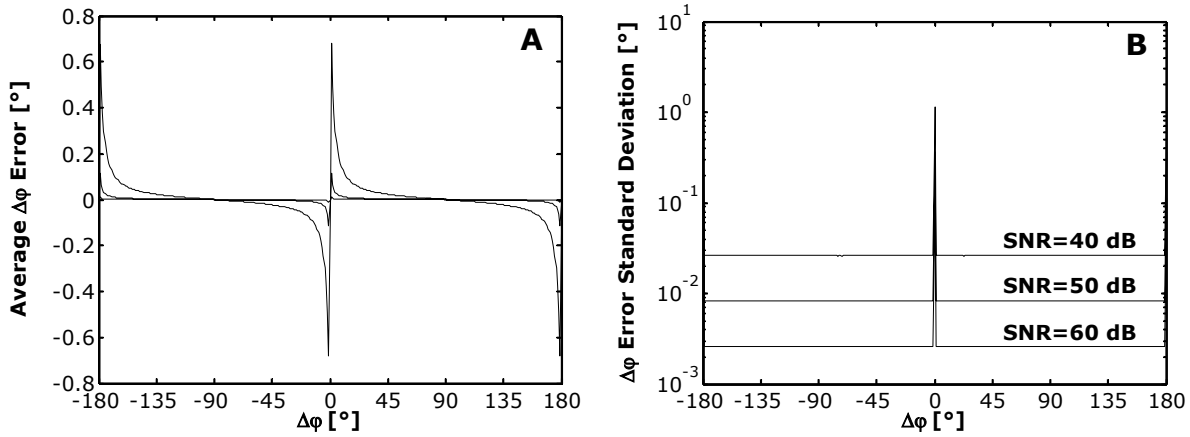

Fig. 11. Average phase difference error (A) and standard deviation (B) for the ellipse fit algorithm as a function of the phase difference and common SNR for D_1=1 V and D_2=0.5 V.

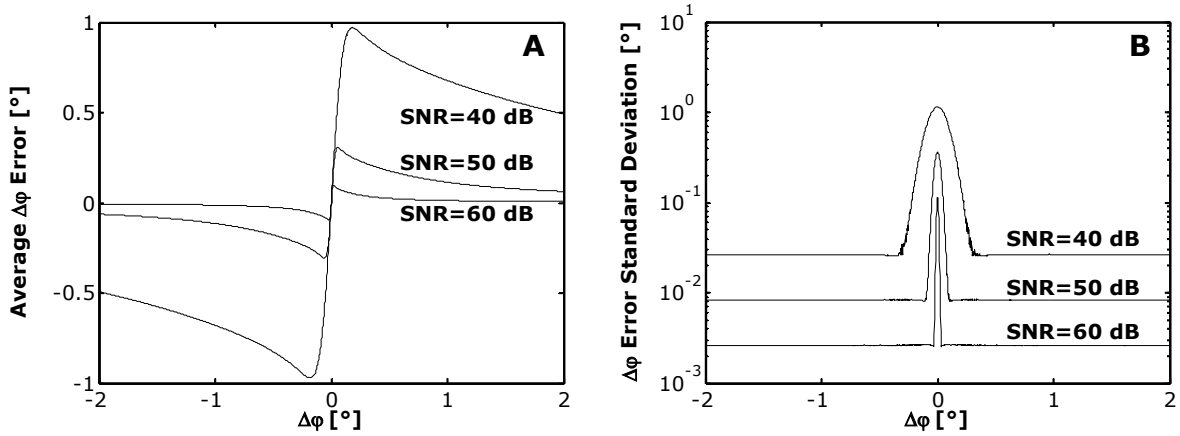

Fig. 12. Detailed view of Fig. 11 near Δφ=0º.

Table 1. Comparison of the algorithms for Δφ=90º.

		$SNR_1=SNR_2$		
		30 dB	45 dB	60 dB
Ellipse fit	D_2/D_1 relative standard deviation	1.5×10^{-3}	2.6×10^{-4}	4.6×10^{-5}
	Phase difference standard deviation [°]	8.3×10^{-2}	1.5×10^{-2}	2.6×10^{-3}
Seven parameter sine fit	D_2/D_1 relative standard deviation	1.0×10^{-3}	1.8×10^{-4}	3.2×10^{-5}
	Phase difference standard deviation [°]	5.8×10^{-2}	1.0×10^{-2}	1.8×10^{-3}
Spectral sinc fit	D_2/D_1 relative standard deviation	1.0×10^{-3}	1.8×10^{-4}	3.2×10^{-5}
	Phase difference standard deviation [°]	5.9×10^{-2}	1.0×10^{-2}	1.8×10^{-3}
Cramér-Rao bound	D_2/D_1 relative standard deviation	1.0×10^{-3}	1.8×10^{-4}	3.2×10^{-5}
	Phase difference standard deviation [°]	5.8×10^{-2}	1.0×10^{-2}	1.8×10^{-3}

Note that the results from the seven-parameter sine fit are identical to the ones obtained with the spectral sinc fit and also identical to the Cramér-Rao lower bound. The results of the ellipse fit are slightly worse.

4. Measurement results

In this section, the measurement results are presented. A Tektronix AFG 3022 function generator was used to generate signals with a frequency $f = 1$ kHz, amplitudes $D_1 = 8$ V and $D_2 = 2$ V and phase shift $\Delta\varphi = 25°$. Two Agilent 33210A generators were used to add random Gaussian noise to these signals. The resulting signals were acquired using the NI USB-9215A data acquisition board (simultaneous sampling, 16 bit, input range ±10V), whose sampling rate was set to 96 kS/s. The acquired signals were then processed using the three estimation algorithms.

In the following test, signals with different settings of SNR were used. The acquired signals were divided into 1 000 frames whose length was set to 288 samples (3 periods) and 1920 samples (20 periods). The ellipse fit, the seven-parameter sine fit and the spectral sinc fit were then used to estimate the signals' parameters in each frame. From these results, the standard deviations of estimation of the signal's parameters were calculated. The relative standard deviation of the amplitude ratio (D_2/D_1) estimation error and the standard deviation of the phase difference $\Delta\varphi$ estimation error are shown in Table 2 while the standard deviation of the frequency estimation error is shown in Table 3.

Table 2. Measurement results – comparison of the algorithms.

		Ellipse fit		**Seven parameter sine fit**		**Spectral sinc fit**	
		D_2/D_1 relative standard deviation	Phase difference standard deviation [°]	D_2/D_1 relative standard deviation	Phase difference standard deviation [°]	D_2/D_1 relative standard deviation	Phase difference standard deviation [°]
N = 288	SNR_1 = 68 dB SNR_2 = 49 dB	5.6×10^{-4}	1.8×10^{-3}	3.4×10^{-5}	2.8×10^{-5}	3.4×10^{-5}	2.8×10^{-5}
	SNR_1 = 53 dB SNR_2 = 41 dB	3.6×10^{-3}	4.3×10^{-2}	5.3×10^{-4}	5.2×10^{-4}	5.3×10^{-4}	5.2×10^{-4}
	SNR_1 = 42 dB SNR_2 = 30 dB	1.3×10^{-2}	1.6×10^{-1}	2.0×10^{-3}	2.0×10^{-3}	2.0×10^{-3}	2.0×10^{-3}
	SNR_1 = 64 dB SNR_2 = 30 dB	1.2×10^{-2}	1.5×10^{-1}	1.8×10^{-3}	1.9×10^{-3}	1.8×10^{-3}	1.9×10^{-3}
N = 1920	SNR_1 = 68 dB SNR_2 = 49 dB	4.0×10^{-4}	5.4×10^{-4}	1.4×10^{-5}	6.3×10^{-6}	1.4×10^{-5}	6.3×10^{-6}
	SNR_1 = 53 dB SNR_2 = 41 dB	1.5×10^{-3}	1.6×10^{-2}	2.0×10^{-4}	2.0×10^{-4}	2.0×10^{-4}	2.0×10^{-4}
	SNR_1 = 42 dB SNR_2 = 30 dB	5.2×10^{-3}	6.2×10^{-2}	8.0×10^{-4}	7.7×10^{-4}	8.0×10^{-4}	7.7×10^{-4}
	SNR_1 = 64 dB SNR_2 = 30 dB	4.8×10^{-3}	6.0×10^{-2}	7.1×10^{-4}	7.8×10^{-4}	7.1×10^{-4}	7.8×10^{-4}

In the following measurement, signals with $SNR_1 = 58$ dB and $SNR_2 = 45$ dB were acquired. The acquired data were divided into 1 000 frames whose length was set from 192 samples (2 periods of the signal) up to 1920 samples (20 periods) in order to investigate the influence of the frame length *N* on the estimation results. The relative standard deviation of the amplitude ratio (D_2/D_1) estimation error and the standard deviation of the phase difference $\Delta\varphi$ estimation error are shown in Fig. 13 and the standard deviation of the frequency estimation error is shown in Fig. 14.

Table 3. Measurement results – frequency estimation.

		Seven parameter sine fit Std. deviation of frequency estimation error [Hz]	Spectral sinc fit Std. deviation of frequency estimation error [Hz]
N = 288	SNR_1 = 68 dB SNR_2 = 49 dB	1.5×10^{-3}	1.2×10^{-3}
	SNR_1 = 53 dB SNR_2 = 41 dB	2.4×10^{-2}	2.9×10^{-2}
	SNR_1 = 42 dB SNR_2 = 30 dB	8.4×10^{-2}	1.1×10^{-1}
	SNR_1 = 64 dB SNR_2 = 30 dB	2.1×10^{-2}	2.8×10^{-3}
N = 1920	SNR_1 = 68 dB SNR_2 = 49 dB	1.0×10^{-4}	1.5×10^{-4}
	SNR_1 = 53 dB SNR_2 = 41 dB	1.4×10^{-3}	1.7×10^{-3}
	SNR_1 = 42 dB SNR_2 = 30 dB	4.9×10^{-3}	6.2×10^{-3}
	SNR_1 = 64 dB SNR_2 = 30 dB	1.2×10^{-3}	2.1×10^{-4}

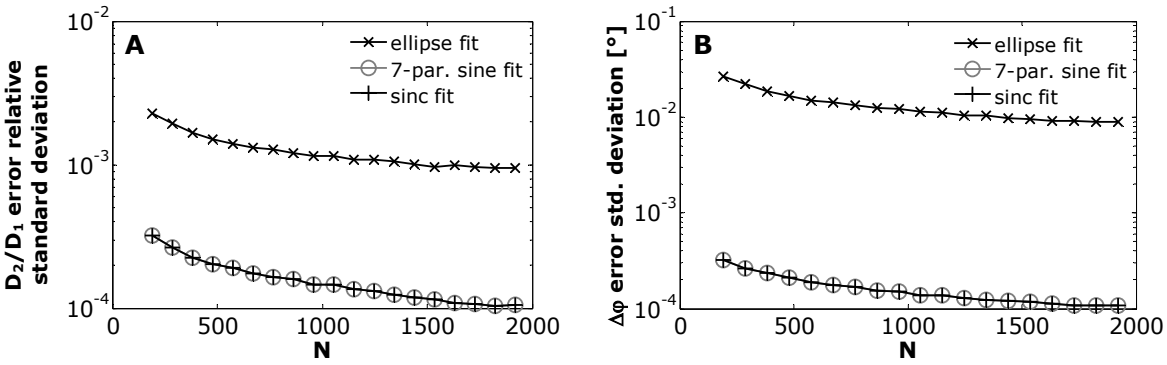

Fig. 13. Measurement results – relative standard deviation of the amplitude ratio (A) and standard deviation of the phase difference error (B) as a function of signal length N.

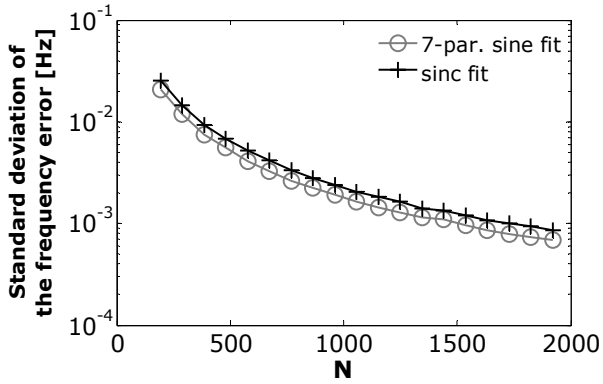

Fig. 14. Measurement results – standard deviation of the frequency estimate error as a function of signal length N.

The measurement results confirm the simulation results. In the considered situations, the results provided by the seven-parameter sine fit and the sinc fit are almost identical (the respective plots are on top of each other in Fig. 13). In cases where the difference between the

two signals' SNRs is significantly different (*e.g.*, the case of $SNR_1 = 64$ dB and $SNR_2 = 30$ dB shown in Table 2 and Table 3) the sinc fit algorithm, thanks to its use of weights, provides significantly better estimates of the frequency than the seven-parameter sine fit (see Table 3). The estimates of the rest of the parameters remain comparable, which is in accordance with the behavior shown in Fig. 6, Fig. 7 and Fig. 8.

The results of the ellipse fit were worse than the results of the other two algorithms, mainly in the case of the phase difference estimate.

5. Conclusions

In this paper the performance of three algorithms for two-channel sinewave parameter estimation was analyzed in a broad range of situations. The two sinewaves have a common frequency since this is the case in many applications. The three compared algorithms were ellipse fit, seven-parameter sine fit and spectral sinc fit.

After the general description of the three algorithms, presented with some detail regarding their implementation, numerical simulations were used to assess and compare the algorithms performance. The parameters used to evaluate this performance were the relative standard deviation of the amplitude ratio error and the standard deviation of the phase difference error. Since the ellipse fit algorithm does not estimate the frequency, the standard deviation of the frequency error was only analyzed for the sine fit and sinc fit algorithms.

The first analysis considered the effect of the signal to noise ratio on the parameters estimated by each algorithm. In this case, for the ellipse fit algorithm, the average of the amplitude ratio error was also presented, confirming the fact that this algorithm is biased for low values of the SNR, while no bias effect was found in the phase difference estimation. The standard deviation of both amplitude ratio error and phase difference error decrease with increasing SNR as expected. The standard deviation results for the sine fit and sinc fit algorithms resemble the ellipse fit results but with lower values, indicating that both algorithms perform better than the ellipse fit. Although the sine fit and sinc fit yielded almost identical results for the amplitude ratio and phase difference analysis, the frequency error analysis shows that the sinc fit performs better when there is a difference in the SNR values of the two signals. This is due to the use of weights in the sinc fit algorithm which gives more relevance to the data in the channel with higher SNR.

The effect of the amplitude of each signal was analyzed next with a fixed, but different, SNR for each signal. It was found that the amplitude ratio error and phase difference error standard deviations are independent of the signal amplitudes. Also, as in the SNR analysis, the sinc fit and sine fit algorithms perform almost identically while the ellipse fit results are slightly worse.

In the phase analysis, emphasis was given on the ellipse fit algorithm due to the known limitations of this algorithm for in-phase and opposition sinewaves which make the ellipse degenerate into line segments. Although the algorithm has difficulties in these situations, it still manages to correctly estimate the amplitude ratio. The sine fit and sinc fit algorithms perform equally well and are very near the Cramér-Rao lower bound.

The evaluation of the three algorithms was complemented with measurement results. The acquisitions were performed with different record lengths to show the influence of the number of acquired samples on the performance of each algorithm. The algorithms perform better as the SNR increases and also as the number of samples increases. The sine fit and sinc fit algorithms performed identically while the ellipse fit results confirm that it performs slightly worse especially in the phase difference estimation.

To conclude, the sine fit and sinc fit algorithms perform equally well and are near the Cramér-Rao lower bound. The sinc fit is slightly better in the frequency estimation, for

different SNRs of the signals. The ellipse fit, despite being fast and non-iterative, performs worse that the other two algorithms, especially where the phase difference is concerned.

Acknowledgments

This work was sponsored by the Fundação para a Ciência e Tecnologia under project PTDC/EEA-ELC/72875/2006.

References

[1] *IEEE Standard for Digitizing Waveform Records*, 2007. IEEE Std. 1057-2007.

[2] P.M. Ramos, M. Fonseca da Silva, A. Cruz Serra: "Low frequency impedance measurement using sine-fitting". *Measurement,* vol. 35, no.1, Jan. 2004, pp. 89–96,

[3] A.L. Ribeiro, H.G. Ramos: "Inductive probe for flaw detection in non-magnetic metallic plates using eddy currents". *IEEE International Instrumentation and Measurement Technology Conference*, Victoria, Canada, May 2008, pp. 1447–1451.

[4] P. Händel, A. Høst-Madsen: "Estimation of velocity and size of particles from two channel laser anemometry measurements". *Measurement*, vol. 21, no. 3, July 1997, pp. 113–123.

[5] P. Händel, P. Zetterberg: "Receiver I/Q Imbalance: Tone Test, Sensitivity Analysis, and the Universal Software Radio Peripheral". *IEEE Trans. Instr. Meas.*, vol. 59, no. 3, March 2010, pp. 704–714.

[6] D. Agrež: "Power measurement in non-coherent sampling". *Measurement*, vol. 41, no. 3, April 2008, pp. 230–235.

[7] M. Novotný, M. Sedláček: "Measurement of active power by time-domain digital signal processing". *Measurement*, vol. 42, no. 8, October 2009, pp. 1139–1152.

[8] P.M. Ramos, A.C. Serra; "A new sine-fitting algorithm for accurate amplitude and phase measurements in two channel acquisition systems". *Measurement*, vol. 41, no. 2, Feb. 2008, pp. 135–143.

[9] P.M. Ramos, F.M. Janeiro, T. Radil: "Comparison of impedance measurements in a DSP using ellipse-fit and seven-parameter sine-fit algorithms". *Measurement*, vol. 42, no. 9, Nov. 2009, pp. 1370–1379.

[10] R. Halíř, J. Flusser: "Numerically stable direct least squares fitting of ellipses". *Proc. WSCG'98*, University of West Bohemia, Czech Republic, Feb. 1998, pp. 125–132.

[11] P.M. Ramos, F.M. Janeiro, M. Tlemçani, A.C. Serra: "Recent Developments on Impedance Measurements With DSP-Based Ellipse-Fitting Algorithms". *IEEE Trans. Instr. Meas.*, vol. 58, no. 5, May 2009, pp. 1680–1689.

[12] T. Radil, P.M. Ramos, A.C. Serra: "New spectrum leakage correction algorithm for frequency estimation of power system signals". *IEEE Trans. Instr. Meas.*, vol. 58, no. 5, May 2009, pp. 1670–1679.

[13] P. Händel: "Parameter estimation employing a dual-channel sine-wave model under a Gaussian assumption". *IEEE Trans. Instr. Meas.*, vol. 57, no. 8, Aug. 2008, pp. 1661–1669.

[14] A. Fitzgibbon, M. Pilu, R. Fischer: "Direct least squares fitting of ellipses". *13th Intern. Conf. on Pattern Recognition*, Vienna, Austria, Sept. 1996, pp. 253–257.

[15] F.M. Janeiro, P.M. Ramos, M. Tlemçani, A.C. Serra: "Analysis of a non-iterative algorithm for the amplitude and phase difference estimation of two acquired sinewaves". *XVIII IMEKO World Congr.*, Rio de Janeiro, Brazil, Sep. 2006.

[16] H. Renders, J. Schoukens, G. Vilain; "High-accuracy spectrum analysis of sampled discrete frequency signals by analytical leakage compensation". *IEEE Trans. Instr. Meas.*, vol. 33, no. 4, Dec 1984, pp. 287–292.